# Supporting Information

**Tables:**

Table S1

| Entry | Catalyst | Catalyst type and name | Manufacturer |
|---|---|---|---|
| 1 | H-BEA-35 | Zeolite, Beta | Südchemie (now Clariant) |
| 2 | H-BEA-150 | Zeolite, Beta | Südchemie (now Clariant) |
| 3 | $NH_4$-FAU-12 | Zeolite, Faujasite | Alfa Aesar |
| 4 | H-FAU-129 | Zeolite, Faujasite | Degussa (now Evonik Industries) |
| 5 | H-FAU-340 | Zeolite, Faujasite | Degussa (now Evonik Industries) |
| 6 | $NH_4$-MOR-14 | Zeolite, Mordenite | Südchemie (now Clariant) |
| 7 | H-MOR-40 | Zeolite, Mordenite | Südchemie (now Clariant) |
| 8 | $NH_4$-MFI-27 | Zeolite, Pentasil | Südchemie (now Clariant) |
| 9 | H-MFI-90 | Zeolite, Pentasil | Südchemie (now Clariant) |
| 10 | Aerosil 200 | Fumed silica, amorphous | Evonik Industries |
| 11 | Silicalite-1 | Zeolite, Pentasil | -- (synthesis procedure see experimental section) |

**Figures:**

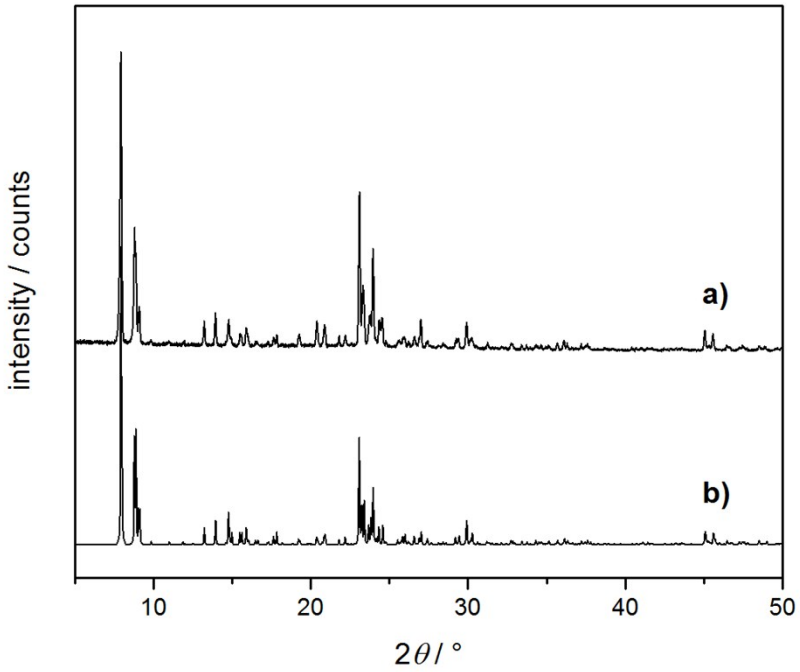


***Figure S2:*** Powder patterns of Silicalite-1: a) experimental and b) calculated using cif-file from http://www.iza-structure.org/databases/ accessed on 22.02.2018.

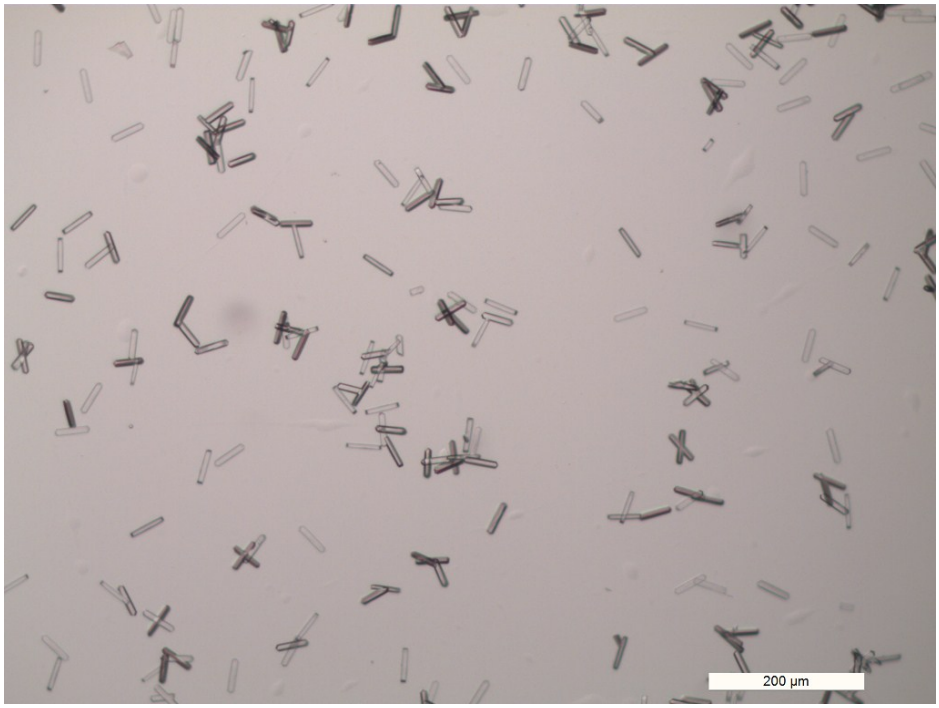


***Figure S3:*** Light microscope image of Silicalite-1 crystals.

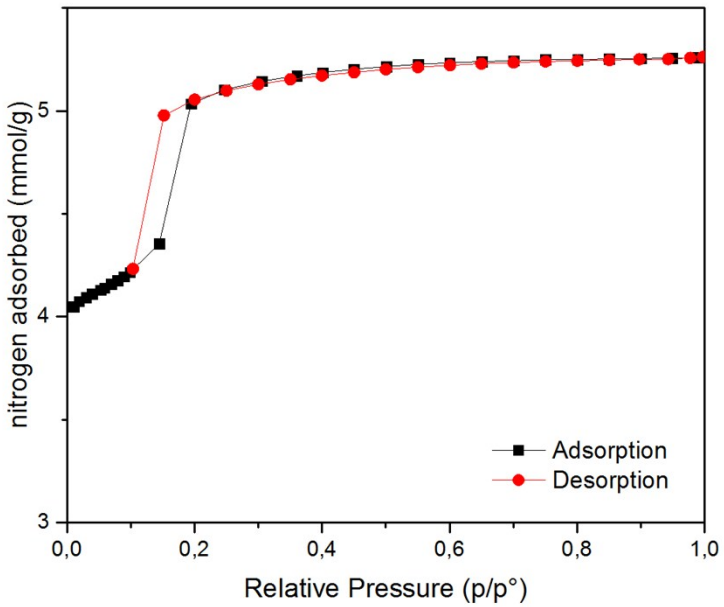


***Figure S4:*** $N_2$-physisorption isotherm of Silicalite-1 crystals. Step and hysteresis of isotherm in the range of $p/p^o$= 0.1 - 0.2 is related to a phase transition of adsorbate molecules inside the micropores as described by Müller and Unger [1].

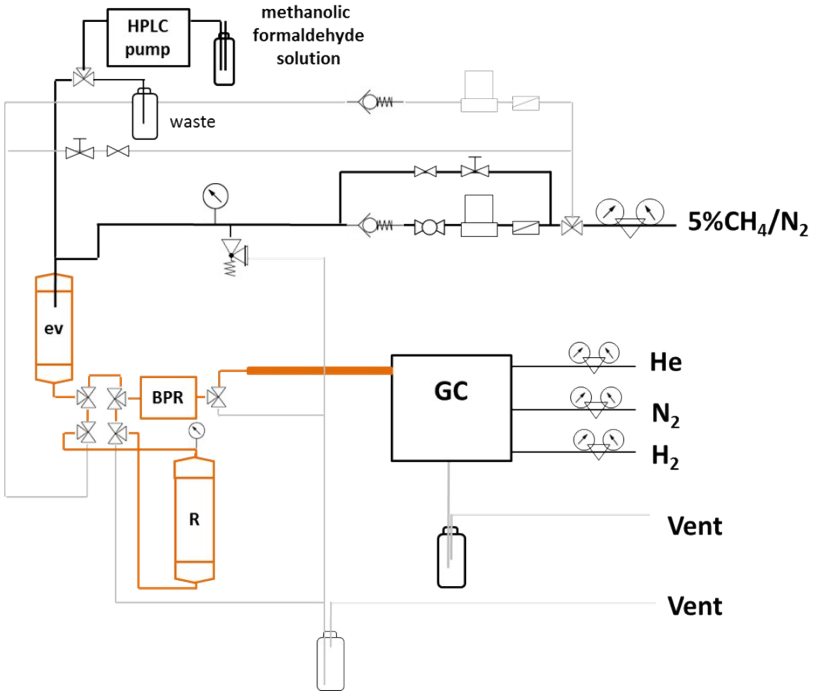


***Figure S5:*** Schematic representation of the set-up used for catalytic tests. Ev: evaporator unit, R: reactor, BPR: back pressure regulator.

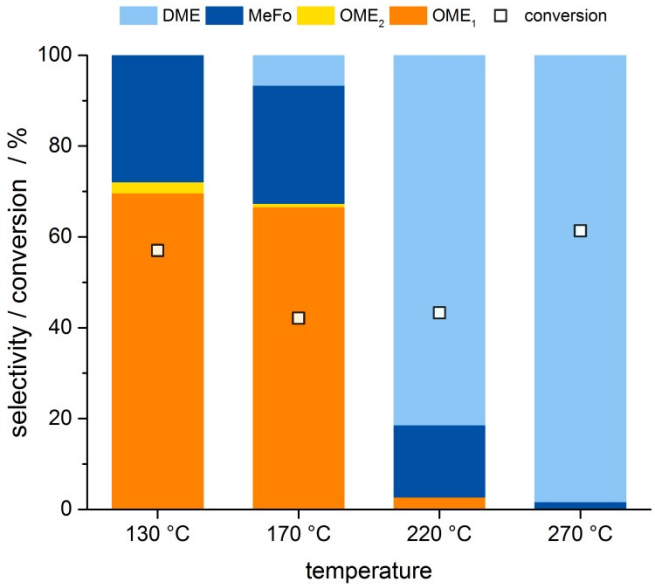


***Figure S6:*** Evaluation of reaction temperature. Reaction conditions: 10 bar, 0.5 g H-MOR-40, 100 mL/min inert gas flow, 14 µL/min FA/MeOH solution feed.

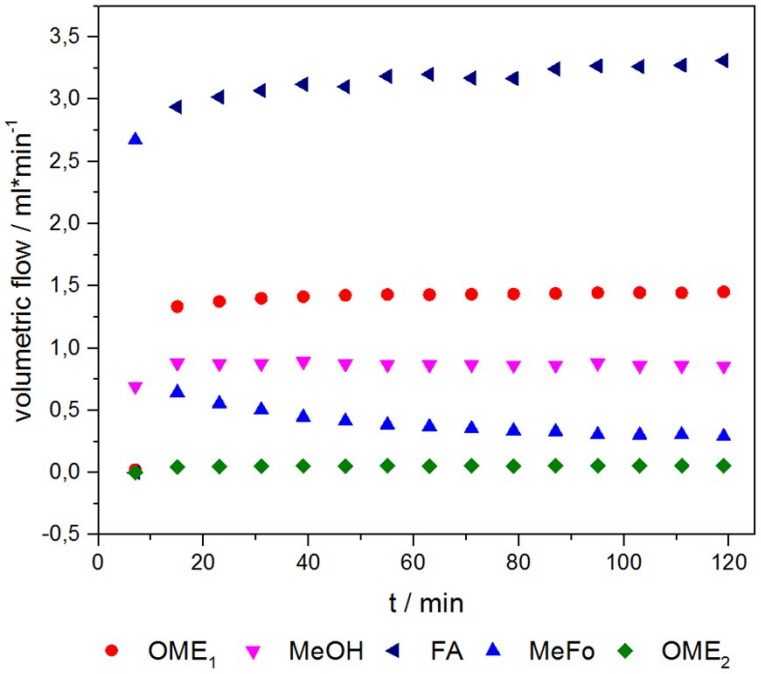


***Figure S7:*** Exemplary product streams for OME synthesis test run over H-MOR-40 showing quasi-plateau after 40 minutes. Reaction conditions: 10 bar, 0.5 g H-MOR-40, 100 mL/min inert gas flow, 14 µL/min FA/MeOH solution feed.

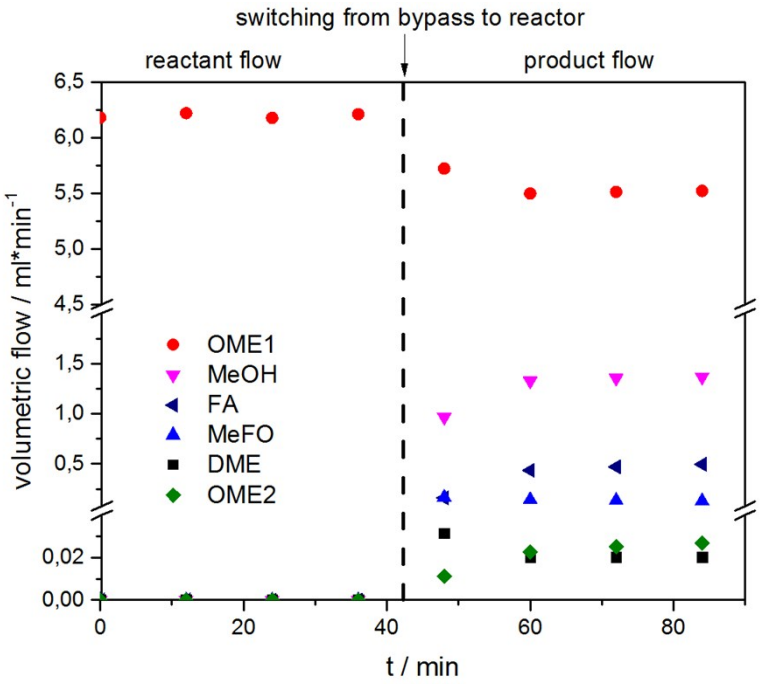


***Figure 8:*** Reversibility test for OME formation. Reaction conditions: 10 bar, 0.5 g H-MOR-40, 100 mL/min inert gas flow, 28 µL/min feed of $OME_1$ + ca. 5 % $H_2O$. $H_2O$ is detected but not quantified.

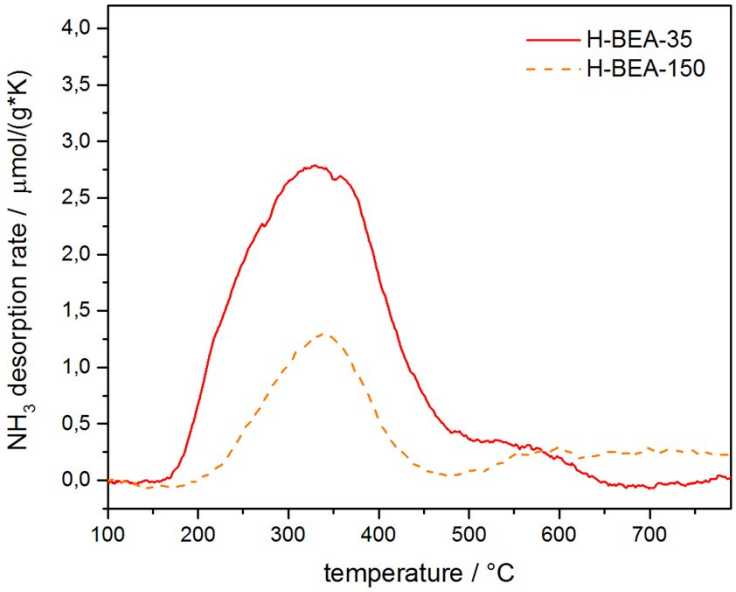


***Figure S9:*** $NH_3$-TPD profiles of H-BEA-35 and H-BEA-150.

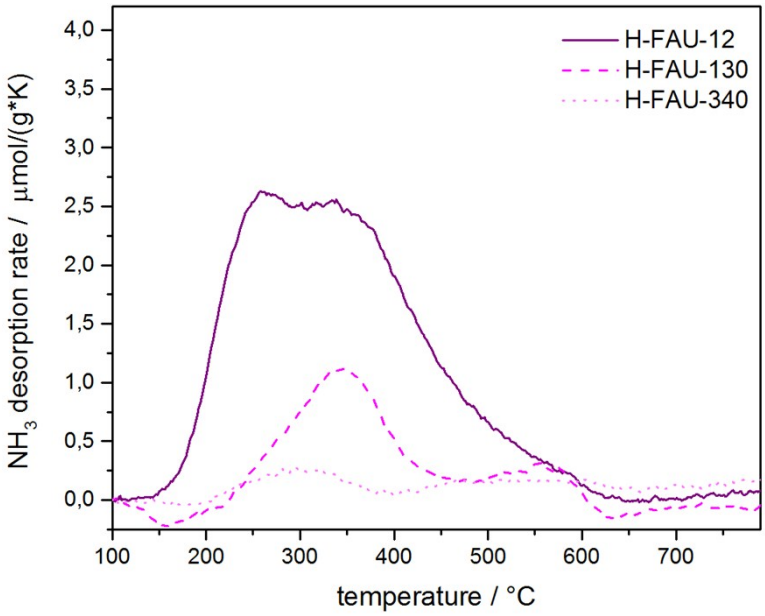


***Figure S10:*** $NH_3$-TPD profiles of H-FAU-12, H-FAU-129 and H-FAU-340.

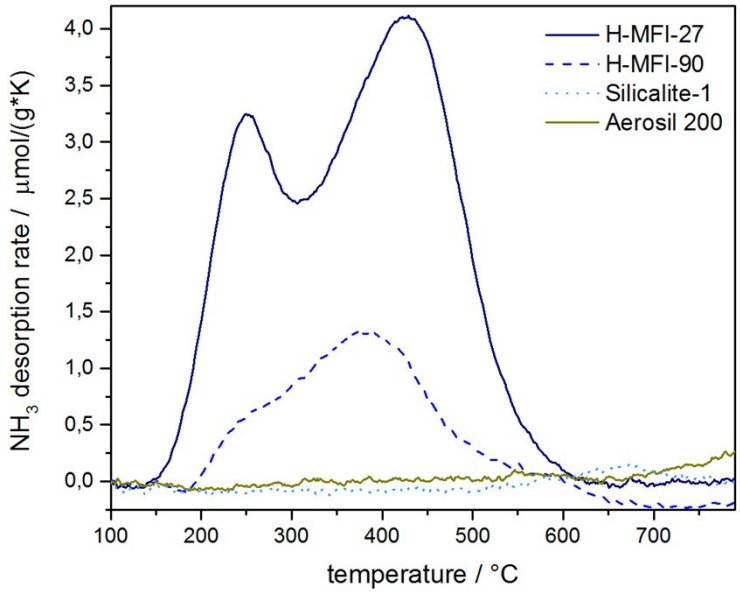


***Figure S11:*** $NH_3$-TPD profile of H-MFI-27, H-MFI-90, Silicalite-1 and Aerosil 200.

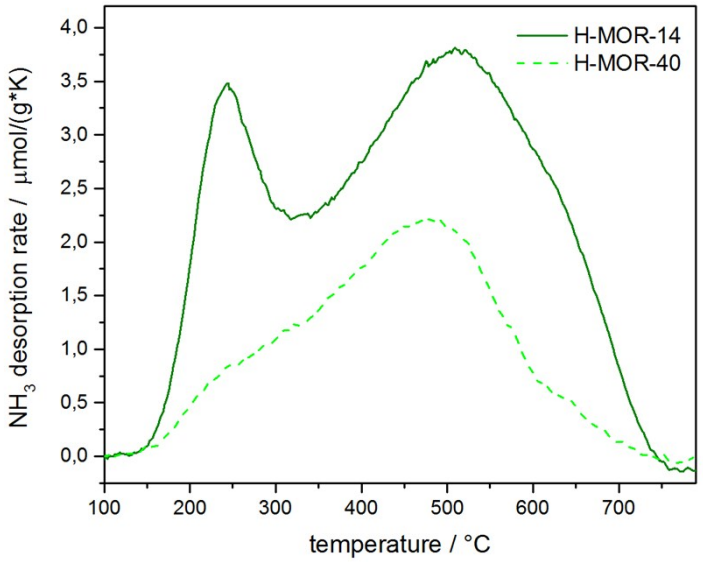


***Figure S12:*** $NH_3$-TPD profile of H-MOR-14 and H-MOR-40.

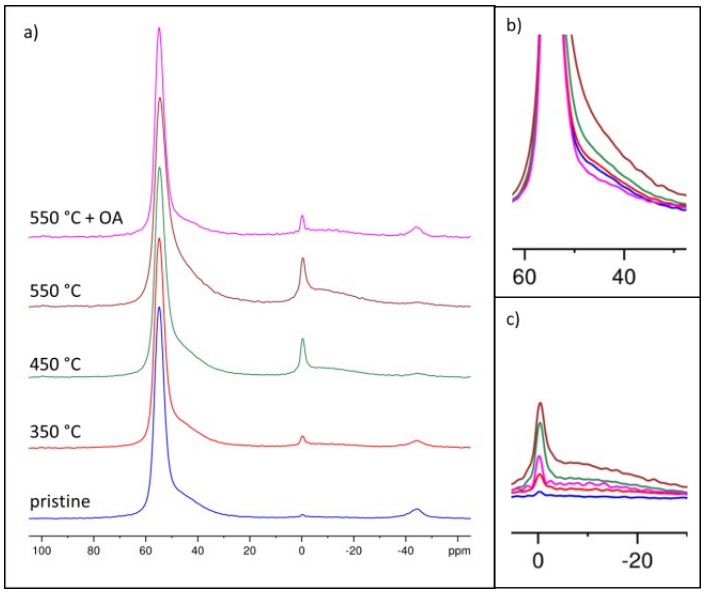


***Figure S13:*** Al-MAS-NMR spectra of H-MOR-40: pristine, calcined at 350 °C, 450 °C, 550 °C and H-MOR-40 calcined at 550 °C with subsequent acid wash using oxalic acid (OA). Stacked spectra (a) and overlapping spectra (b and c). Signals are normalized to the signal at 57 ppm.

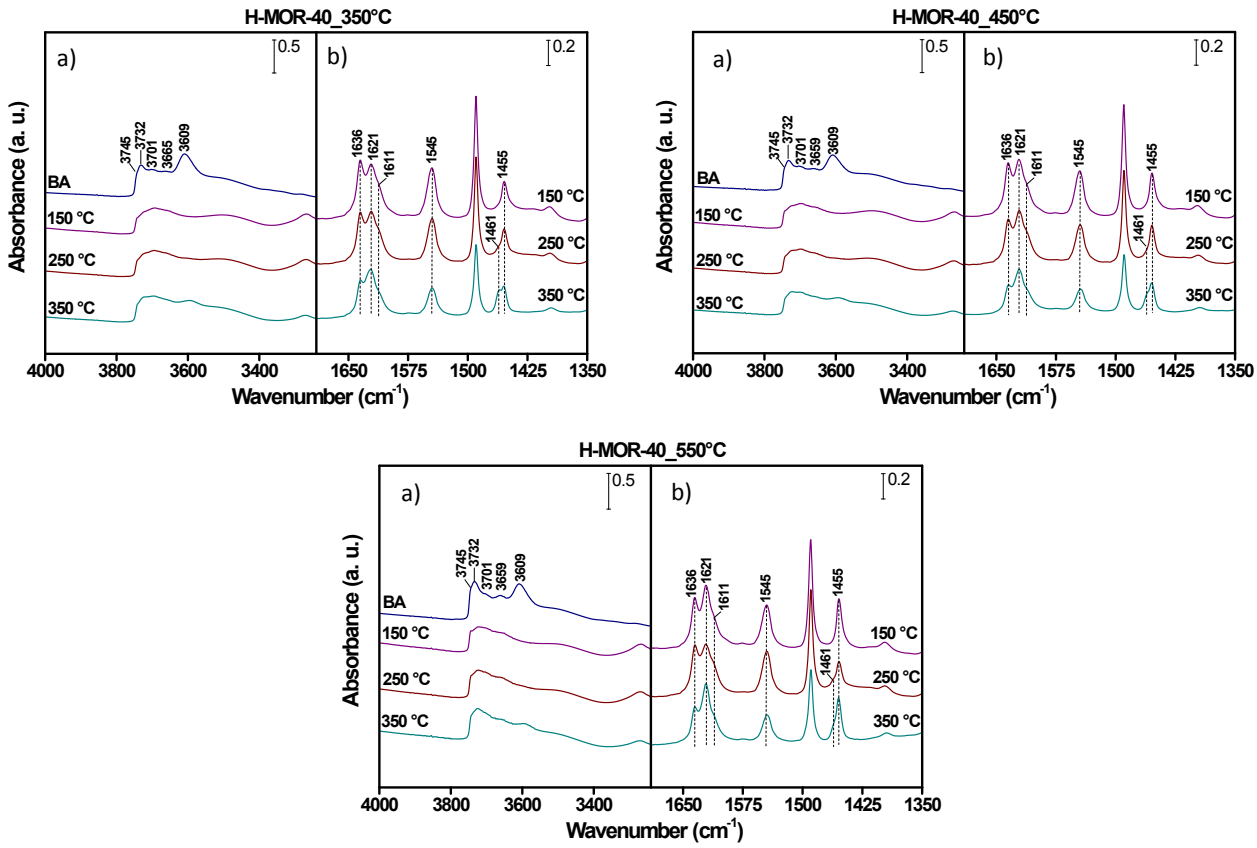


***Figure S14:*** FTIR spectra of the H-MOR-40 at different calcination temperatures after activation by outgassing at 350 °C: a) ν(OH) vibrations and b) stretching vibration region of the pyridine interacting with the acid sites before adsorption (BA) and after 20 min desorption at 150 °C, 250 °C and 350 °C.

In order to get more information about the influence of calcination temperature on the distribution of Brønsted and Lewis acid sites (BAS and LAS, respectively), a pyridine adsorption study was performed. Figure S13 presents the transmission spectra of H-MOR-40 calcined at 350 °C, 450 °C and 550 °C. In the OH stretching vibration region (Figure S13 a), five different absorption bands are observed in the spectra before adsorption (BA) [2, 3]: a) 3745 $cm^{-1}$: characteristic band of terminal silanols, b) 3732 $cm^{-1}$: corresponds to silanols located at internal positions (internal defects), c) 3701 and 3659 $cm^{-1}$: usually associated to OH groups located on extra-framework species and d) 3609 $cm^{-1}$: ascribed to bridging acidic hydroxyl groups (Si-OH-Al). After adsorption of pyridine at 150 °C, the latter bands fade away giving rise to the appearance of new bands in the pyridine vibration region (Figure S13 b). The pyridine interaction with the protons of Brønsted sites leads to typical bands at 1636 and 1545 $cm^{-1}$ characteristic of pyridinium ions ($PyH^+$) [4, 5]. On the other hand, pyridine adsorbed on Lewis acid sites (PyL) is responsible for the band at 1455 $cm^{-1}$, corresponding to the 19b vibration mode of the pyridine. Furthermore, analyzing the 8a vibration mode region is possible to distinguish two different Lewis species at 1621 and 1611 $cm^{-1}$, which can be ascribed to the presence of unsaturated $Al^{3+}$ ions with different environments [6]. In Figure S13 b, a decreased of the band intensities with the temperature due to the existence of acid sites with different strengths is also observed. Besides, the formation of a new band at 1461 $cm^{-1}$ is associated to iminium ions interacting with some PyL complexes [2].

Apparently, the existence of this band depends on calcination temperature and, hence, the presence of acidic protons ($C_{BAS,\ H\text{-}MOR\text{-}40\_350°C} > C_{BAS,\ H\text{-}MOR\text{-}40\_450°C} > C_{BAS,\ H\text{-}MOR\text{-}40\_550°C}$). This fact explains why this band is sharper for the sample calcined at 350 °C (possessing higher initial concentration of BAS and more probabilities that some iminium ions interact with the PyL) than at 450 °C or 550 °C.

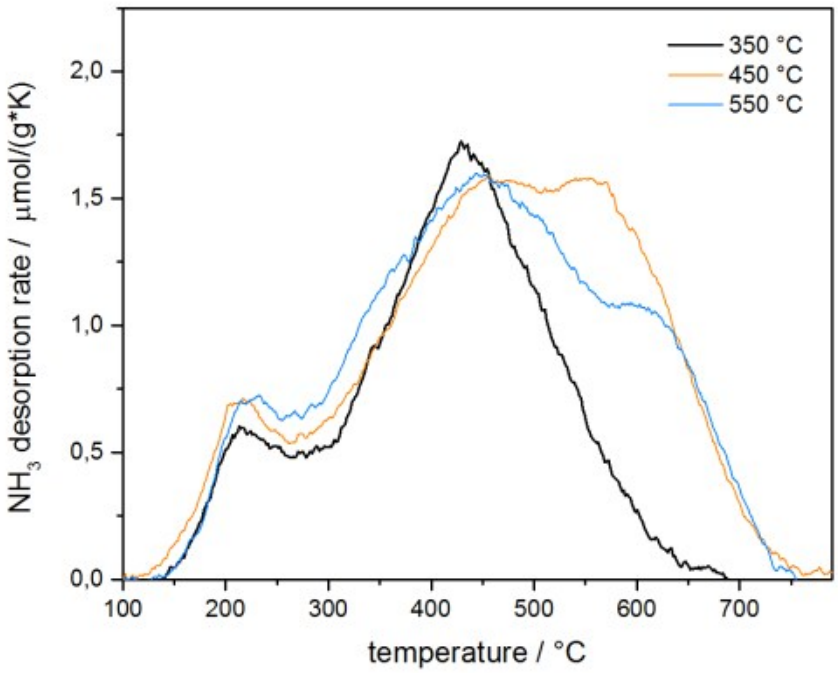


***Figure S15:*** $NH_3$-TPD profiles of H-MOR-40 treated at varying calcination temperatures. In order to not subject the samples to change in EFAl-content, a mild activation procedure was chosen: 100 mg of catalyst were activated at 623 K for 5 h (heating ramp of 2 K $min^{-1}$) and then cooled to 423 K.

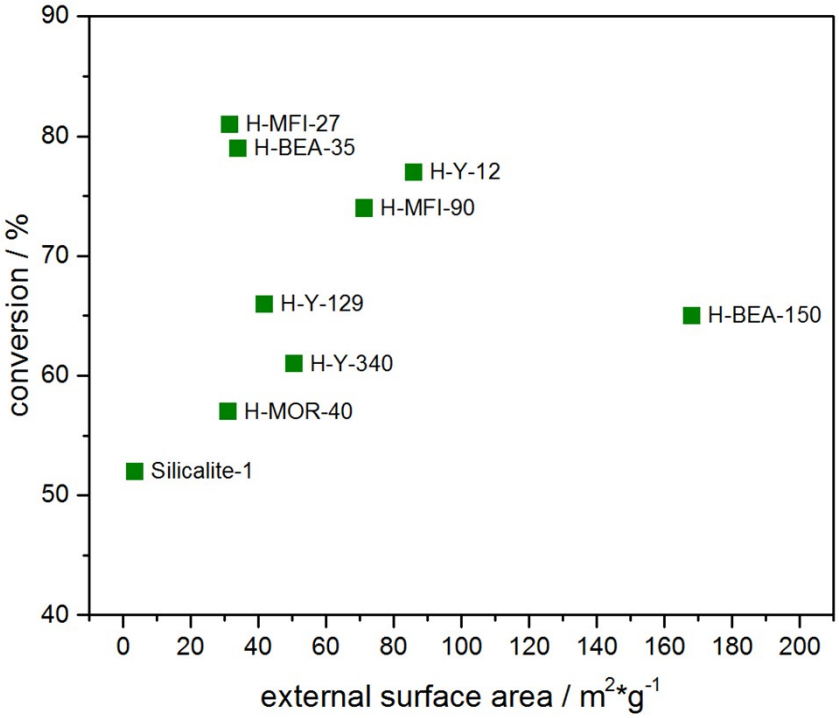


***Figure S16:*** Conversion as a function of external surface area.

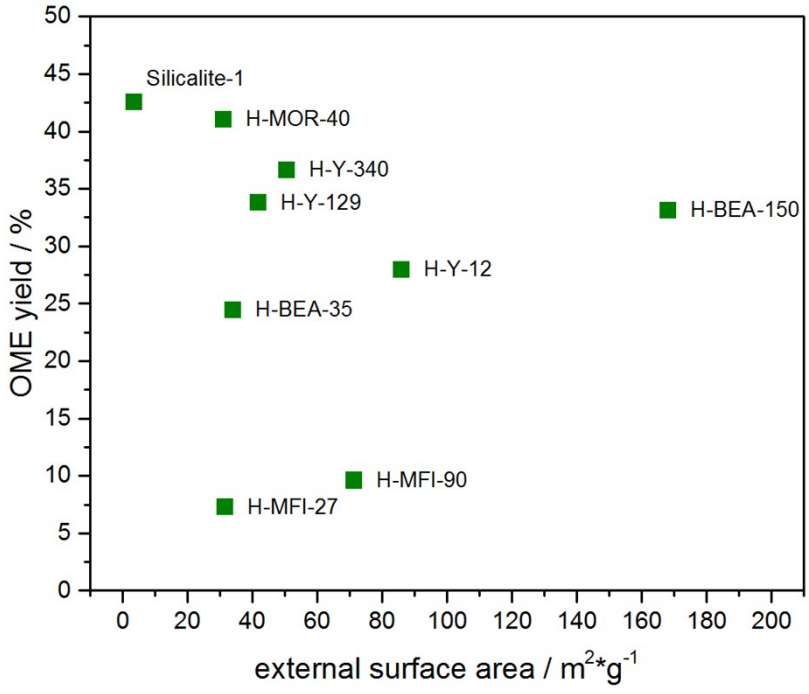


***Figure S17:*** OME yield as a function of external surface area.

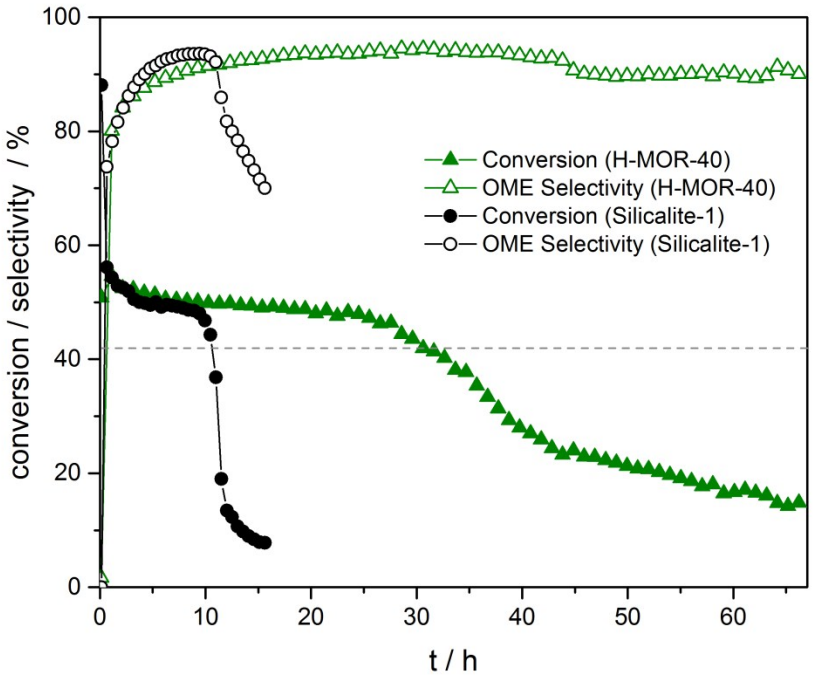


***Figure S18:*** Exemplary deactivation curve: Conversion and OME selectivity as a function of time for H-MOR-40 and Silicalite-1. The defined deactivation onset is indicated as a dotted grey line.

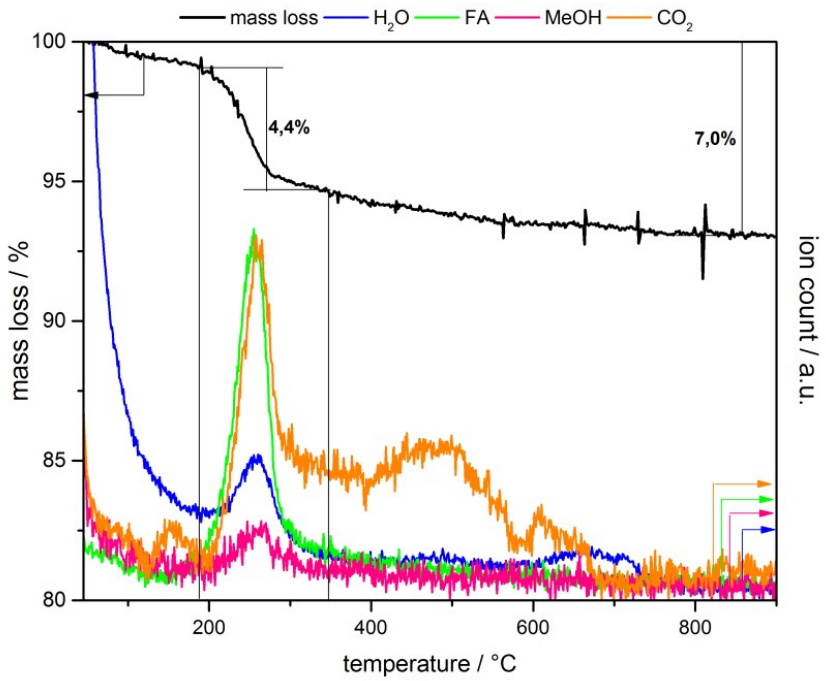


***Figure S19:*** TG-MS curve of Silicalite-1 measured in synthetic air.

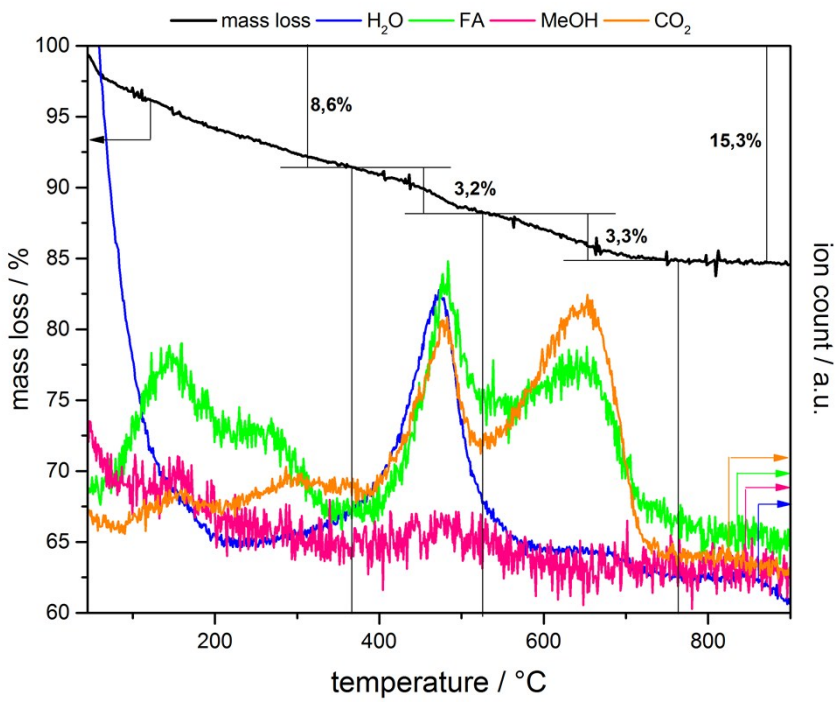


***Figure S29:*** TG-MS curve of H-MOR-40 measured in synthetic air.

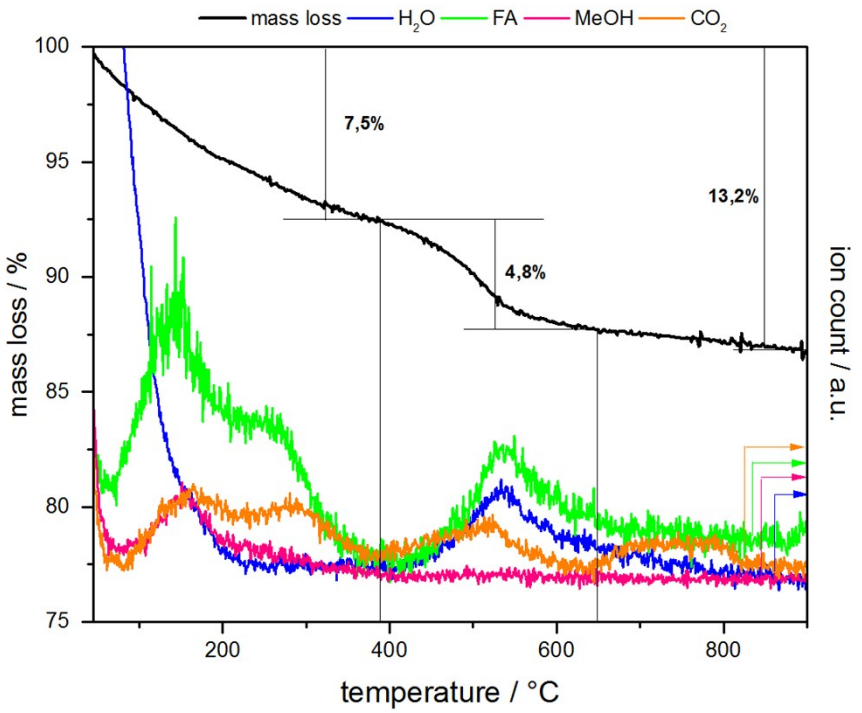


***Figure S21:*** TG-MS curve of H-MOR-40 measured in argon.

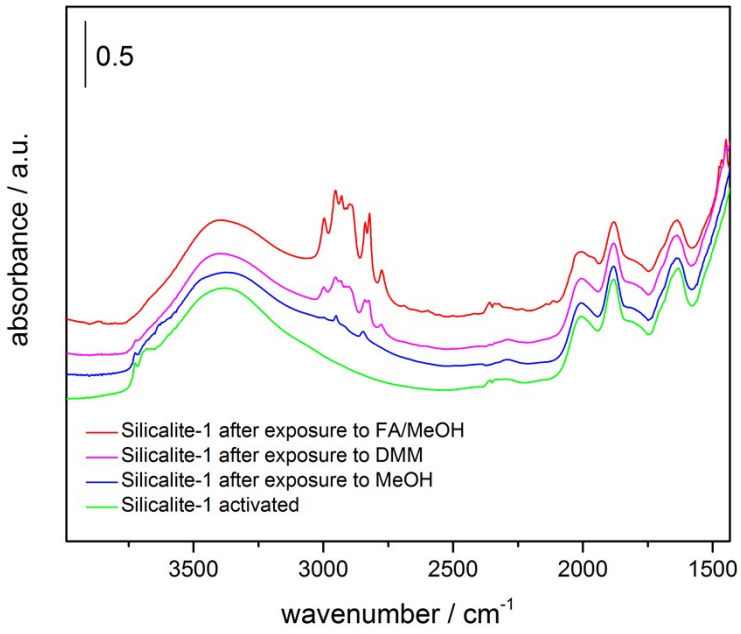


***Figure S22:*** DRIFT-FTIR-spectra of activated Silicalite-1 before and after adsorption of probe molecules.

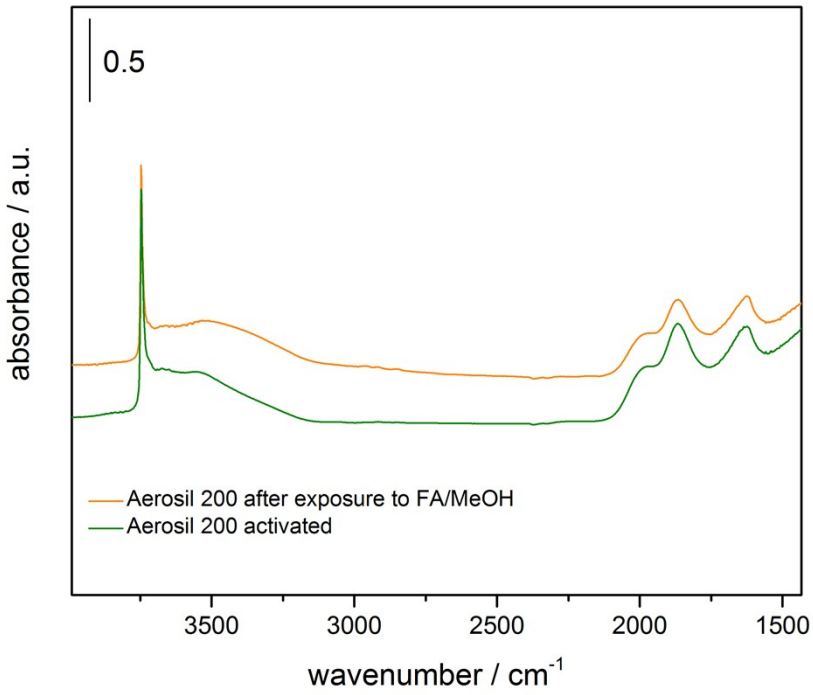


***Figure S23:*** DRIFT-FTIR-spectra of activated Aerosil 200 before and after adsorption of probe molecules.

References

[1] U. Müller and K. K. Unger, in *Studies in Surface Science and Catalysis*, eds. K. K. Unger, J. Rouquerol, K. S. W. Sing and H. Kral, Elsevier, 1988, vol. 39, pp. 101-108.)

[2] B. Gil, S. I. Zones, S.-J. Hwang, M. Bejblová, J. Čejka, J. Phys. Chem. C 2008, 112, 2997-3007.

[3] O. Marie, P. Massiani, F. Thibault-Starzyk, J. Phys. Chem. B 2004, 108, 5073-5081.

[4] J. Fermoso, H. Hernando, P. Jana, I. Moreno, J. Přech, C. Ochoa-Hernández, P. Pizarro, J. M. Coronado, J.Čejka, D. P. Serrano, Catal. Today 2016, 15, 171-181.

[5] G. Busca, Microporous Mesoporous Mater. 2017, 254, 3-16.

[6] C. Poupin, R. Maache, L. Pirault-Roy, R. Brahmi, C.T. Williams, Appl. Catal. A: Gen. 2014, 475, 363-370.